

## Supplementary Materials

### **Efficient degradation of carbamazepine by polydopamine-decorated Co/N@ZS activated peroxymonosulfate: performance and mechanism**

**Yingyi Li<sup>1</sup>, Ziyang Jiang<sup>1</sup>, Shuang Shan<sup>2</sup>, Kairuo Zhu<sup>1</sup>, Chaohai Wang<sup>3,\*</sup>, Rongfu Peng<sup>1,3</sup>, Xianquan Li<sup>2,\*</sup>, Shangru Zhai<sup>1,4,\*</sup>**

<sup>1</sup>Liaoning Key Lab of Lignocellulose Chemistry and BioMaterials, Liaoning Collaborative Innovation Center for Lignocellulosic Biorefinery, School of Light Industry and Chemical Engineering, Dalian Polytechnic University, Dalian 116034, Liaoning, China.

<sup>2</sup>State Key Laboratory of Catalysis, Dalian Institute of Chemical Physics, Chinese Academy of Sciences, Dalian 116023, Liaoning, China.

<sup>3</sup>Henan Key Laboratory of Water Pollution Control and Rehabilitation Technology, School of Municipal and Environmental Engineering, Henan University of Urban Construction, Pingdingshan 467036, Henan, China.

<sup>4</sup>School of Environmental and Nature Resources, Zhejiang University of Science and Technology, Hangzhou 310023, Zhejiang, China.

**\*Correspondence to:** Dr. Xianquan Li, State Key Laboratory of Catalysis, Dalian Institute of Chemical Physics, Chinese Academy of Sciences, Dalian 116023, Liaoning, China. E-mail: [lixianquan@dicp.ac.cn](mailto:lixianquan@dicp.ac.cn); Prof. Shangru Zhai, Liaoning Key Lab of Lignocellulose Chemistry and BioMaterials, Liaoning Collaborative Innovation Center for Lignocellulosic Biorefinery, School of Light Industry and Chemical Engineering, Dalian Polytechnic University, Dalian 116034, Liaoning, China. E-mail: [zhairschem@163.com](mailto:zhairschem@163.com); Prof. Chaohai Wang, Henan Key Laboratory of Water Pollution Control and Rehabilitation Technology, School of Municipal and Environmental Engineering, Henan University of Urban Construction, Pingdingshan 467036, Henan, China. E-mail: [chaohai@huuc.edu.cn](mailto:chaohai@huuc.edu.cn)

### **Supplementary Text 1. Chemical reagents**

Dopamine hydrochloride ( $C_8H_{11}NO_2 \cdot HCl$ , 98%), Polyethylene oxide–polypropylene oxide–polyethylene oxide (P123,  $EO_{20}PO_{70}EO_{20}$ ), Zirconium oxychloride octahydrate ( $ZrOCl_2 \cdot 8H_2O$ ), Tetraethyl orthosilicate (TEOS,  $Si(OC_2H_5)_4$ ), Cobalt nitrate hexahydrate ( $Co(NO_3)_2 \cdot 6H_2O$ , 99%), Carbamazepine (CBZ,  $C_{15}H_{12}N_2O$ ,  $\geq 98.0\%$ ), Norfloxacin (NOR,  $C_{16}H_{18}FN_3O_3$ , 98%), Potassium Peroxymonosulfate (PMS,  $KHSO_5 \cdot 0.5KHSO_4 \cdot 0.5K_2SO_4$ ), Humic acid (HA,  $\geq 90\%$ ), 1, 4-Benzoquinone (p-BQ,  $> 99\%$ ) and L-histidine (L-His,  $> 99\%$ ) were obtained from Shanghai Aladdin Biochemical Technology Co., Ltd (Shanghai, China). Ethanol (EtOH,  $\geq 99.7\%$ ), tert-butanol (TBA,  $\geq 98.0\%$ ) and methanol ( $CH_3OH$ ,  $\geq 99.5\%$ ), Hydrochloric acid (HCl, 36.0~38.0%), Sodium hydroxide (NaOH,  $\geq 96.0\%$ ) were gained from Sinopharm Chemical Reagent Co., Ltd (China). Sodium chloride (NaCl,  $\geq 99.5\%$ ), sodium dihydrogen phosphate ( $NaH_2PO_4$ , 99.5%), sodium bicarbonate ( $NaHCO_3$ ,  $\geq 99.8\%$ ) and sodium nitrate ( $NaNO_3$ ,  $\geq 99.0\%$ ) were supplied by Tianjin Kermel Chemical Reagent Co., Ltd. All of the water used during the experiment was deionized water. All of the chemicals and reagents were of analytical grade and used without further purification.

### **Supplementary Text 2. Synthesis of the Zr-SBA-15 (ZS) and Co/N@ZS**

An ordered mesoporous silica Zr-SBA-15 was synthesized by the procedure described via hydrothermal method. Firstly, 5 g triblock copolymer PEO-PPO-PEO (P123), as a template agent, was added to the conical flask containing the mixed solution of 170 mL deionized water and 30 mL hydrochloric acid with vigorous stirring at  $40^\circ C$  until P123 was completely dissolved. Next, added 0.8 g  $ZrOCl_2 \cdot 8H_2O$  into the solution stirring for 30 minutes, then added 11 mL tetraethyl orthosilicate (TEOS) dropwise. After stirring for 24 hours under the same reaction conditions, the mixture was transferred to a hydrothermal synthesis reactor and kept at  $100^\circ C$  for 24 hours. Finally, collected the products by suction filtering and multiple washing to remove impurities. The pure samples with drying at  $60^\circ C$  for 6 h were calcined at a certain temperature in a muffle furnace for 6 hours.

Co/N@ZS was simply prepared by carbonizing a mixture of  $Co(NO_3)_2 \cdot 6H_2O$ , Zr-SBA-15 and Histidine. Firstly, a mixture of  $Co(NO_3)_2 \cdot 6H_2O$  (0.6 g), ZS (1 g) and Histidine

(1.4 g) was ground for 20 min, and then underwent the calcination at 700°C for 3 h in a tube furnace (at a rate of 5 °C/min) under nitrogen protection. The obtained production was denoted as Co/N@ZS. In contrast, other samples carbonized at the 700°C without the addition of cobalt species was labeled as N@ZS.

### **Supplementary Text 3. Experimental procedure**

The pH value is adjusted with sodium hydroxide and hydrochloric acid. In addition, the influence of coexisting substances ( $\text{Cl}^-$ ,  $\text{H}_2\text{PO}_4^-$ ,  $\text{HCO}_3^-$ ,  $\text{NO}_3^-$ , HA) on the degradation process was investigated. During the quenching experiments, the primary reactive oxygen species (ROS) consisted of various quenchers, namely tert-butanol (TBA), ethanol (EtOH), L-histidine (L-His), Potassium iodide (KI), and 1,4-benzoquinone (p-BQ). To demonstrate reusability, they were recovered by centrifugation and washed with deionized water, then dried in a vacuum oven (60°C). Each experiment was performed in triplicate, with error bars indicating the standard deviation of the results.

### **Supplementary Text 4. Analytical methods**

The as-synthesized samples were subjected to analysis of their microscopic morphology using field-emission scanning electron microscopy (FESEM, JSM-7800F) and high-resolution transmission electron microscopy (HRTEM, JEM-2100F, JEOL). The element distribution was performed at Energy-dispersive X-ray spectroscopy (EDS, X-Max50, Oxford, UK). The crystal structure of the samples was determined by analyzing the X-ray diffraction (XRD) patterns using a Shimadzu XRD-7000s instrument. The surface functional groups of the catalysts were measured using Fourier-transform infrared spectroscopy (FT-IR; Nicolet IS 50, USA). The Brunauer, Emmett and Teller (BET) specific surface area test and  $\text{N}_2$  adsorption-desorption isotherms were monitored via the JW-BK222 analyzer to gain the pore structure and surface area of the materials. The surface chemical state was analyzed using the X-ray photoelectron spectrum (XPS, ESCALAB 250Xi). The leaching of cobalt was detected through atomic absorption spectrophotometry (AAS, ZA3300). Electron Spin Resonance Spectroscopy (EPR; Bruker EMX-plus, Germany) was employed for the detection of active free radicals, in combination with quenching experiments, to summarize the degradation mechanism. HPLC-mass spectroscopy (MS) (RRHD SB-C18, 2.1×100 mm, 1.8 μm, Agilent, USA) was utilized to identify intermediate products and infer the degradation pathways. The residual CBZ concentration after

degradation was measured by high performance liquid chromatograph (HPLC, Agilent, USA). The Column - BEH C18 (2.1×100 mm, 1.7 μm) was used for HPLC. The eluent consisted of two mobile phases at 0.4 mL/min: (A) 0.1% formic acid in water (v/v) and (B) 0.1% formic acid in acetonitrile. The gradient was as follows: component A was maintained at 95% during the first 8 min, then B was increased from 5% to 100 % in the next 4.5 min and B was maintained at 95 % in the final 7.5 min. The mass spectrometric analysis was conducted using positive/ negative electrospray ionization with a mass scan range of m/z 50-1000. The capillary voltage, cone voltage, desolvation temperature, and source temperature were set at 2000 V, 40 V, 450°C, and 115°C, respectively.

The electrochemical workstations (CHI660, China) were utilized to conduct Linear Sweep Voltammetry (LSV), Open Circuit Potential Transients (OCPT), and Electrochemical Impedance Spectroscopy (EIS) tests. All electrochemical tests were performed using a standard three-electrode cell (glassy carbon electrode as the working electrode, Ag/AgCl (4 M KCl) as a reference electrode and platinum electrode as a counter electrode). The 0.5 M of Na<sub>2</sub>SO<sub>4</sub> (0.30 g/L PMS and 20 mg/L CBZ) was selected as electrolyte solution. Firstly, the mixture of 10 mg of catalyst, 0.2 mL of Nafion (5 wt%) and 2 mL EtOH was sonicated for an hour. Afterwards, the mixture (20 μL) was dropped on the glassy carbon electrode and dried in a 60°C vacuum oven. Electrochemical impedance spectra (EIS) were monitored at 0.28 V vs. Ag/AgCl from 0.01 to 10000 Hz at a 5 mV amplitude. Linear sweep voltammograms were tested from -2.0 to 2.0 V at a scan rate of 20 mV/ S.

**Supplementary Table 1. HPLC analytical methods for Different Compounds**

<b>Compound</b>	<b>Detection wavelength (λ, nm)</b>	<b>Flow (mL/min)</b>	<b>ultrapure water</b>	<b>For-mic acid</b>	<b>Aceto-nitrile</b>	<b>ultrapure water (0.2% trifluoroacetic acid)</b>
carbamazepine	285	0.8	40%	/	60%	/
ciprofloxacin	278	0.1	/	70%	30%	/

tetracycline	358	0.3	/	90%	10%	/
Norfloxacin	278	1.5	/	40%	5%	55%

**Supplementary Tables 2. The EDS results of (A) Co/N@ZS and (B) Co/N@ZS-PDA**

(A)

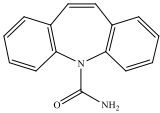
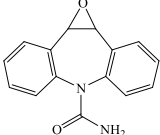
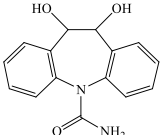
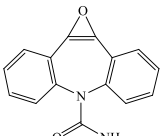
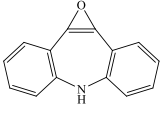
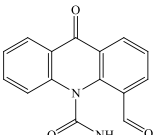
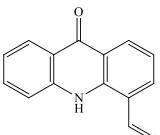
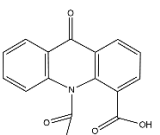
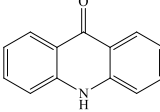
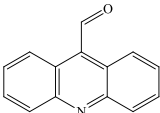
Element	Apparent Concentration	k Ratio	Wt%	Atomic %
C	17.05	0.17047	47.07	59.86
N	3.31	0.00589	3.82	4.16
O	24.07	0.08101	29.15	27.83
Si	15.78	0.12503	11.88	6.46
Co	3.62	0.03622	3.61	0.94
Zr	4.22	0.04218	4.47	0.75
Total:			100.00	100.00

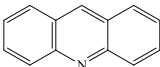
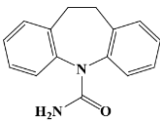
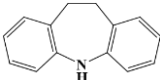
(B)

Element	Apparent Concentration	k Ratio	Wt%	Atomic %
C	11.90	0.11898	38.95	50.72
N	6.55	0.01165	6.83	7.63
O	26.82	0.09024	32.21	31.49
Si	21.12	0.16733	16.10	8.96
Co	1.93	0.01926	1.96	0.52
Zr	3.54	0.03536	3.94	0.68
Total:			100.00	100.00

**Supplementary Table 3. CBZ and possible intermediates detected by LC-MS**

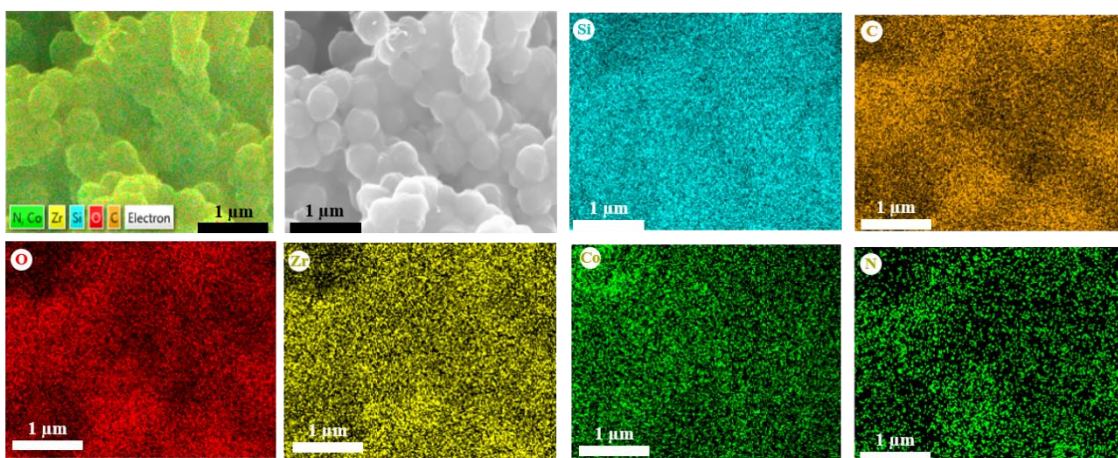
Product	m/z	Molecular formula	Proposed structure
---------	-----	-------------------	--------------------

CBZ	+237	C <sub>15</sub> H <sub>12</sub> N <sub>2</sub> O	
P1	+253	C <sub>15</sub> H <sub>12</sub> N <sub>2</sub> O <sub>2</sub>	
P2	+271	C <sub>15</sub> H <sub>14</sub> N <sub>2</sub> O <sub>3</sub>	
P3	+ 251	C <sub>15</sub> H <sub>10</sub> N <sub>2</sub> O <sub>2</sub>	
P4	+ 208	C <sub>14</sub> H <sub>9</sub> NO	
P5	+267	C <sub>15</sub> H <sub>10</sub> N <sub>2</sub> O <sub>3</sub>	
P6	+ 224	C <sub>14</sub> H <sub>9</sub> NO <sub>2</sub>	
P7	+283	C <sub>15</sub> H <sub>10</sub> N <sub>2</sub> O <sub>4</sub>	
Product	m/z	Molecular formula	Proposed structure
P8	+196	C <sub>13</sub> H <sub>9</sub> NO	
P9	+ 208	C <sub>14</sub> H <sub>9</sub> NO	

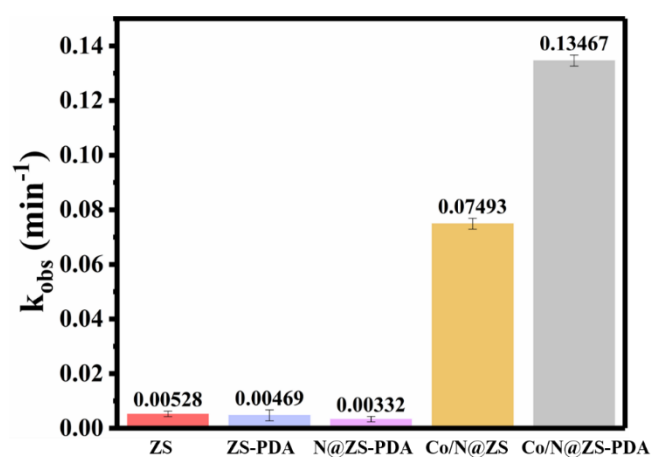
P10	+180	C <sub>13</sub> H <sub>9</sub> N	
P11	+240	C <sub>15</sub> H <sub>14</sub> N <sub>2</sub> O	
P12	+196	C <sub>14</sub> H <sub>13</sub> N	

**Supplementary Table 4. Performance comparison of different catalysts for PMS activation**

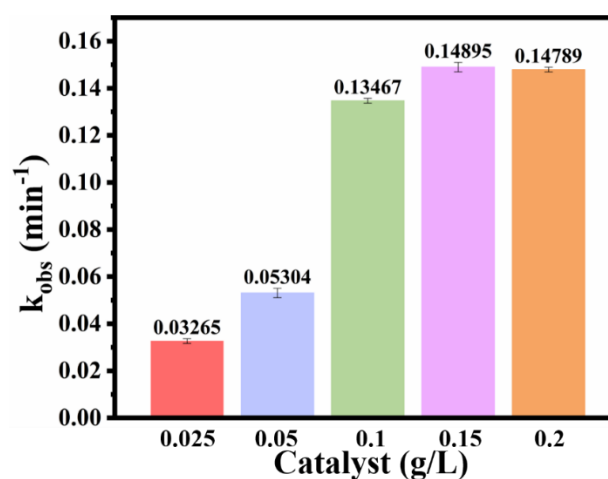
Catalyst	Pollutant	Concentration of pollutant (mg/L)	Catalyst dosage	PMS dosage	Removal efficiency (%)	Continuous flow rate time (h)	Continuous flow rate (mL/min)	Ref.
Co-OCN	APAP	0.1	0.05 g	0.5 mM	85	36	2	[1]
BFO/BNQDs@PE TC-HCl		5	0.09 g	1 mM	70	7	0.3	[2]
SA/PEI-Co <sub>x</sub> O <sub>y</sub>	MB	100	0.6 g	1.2 g/L	90.26	6.67	1	[3]
Co-NC-0.25-700°C	MB	240	0.2 g	6 mM	80	1	1	[4]
CoAl-Aaps-600	PNP	10	20 g	0.4 g/L	60	8	10	[5]
Co/N@ZS-PDA	CBZ	20	0.1 g	0.3 g/L	95.80	160	0.1	this work



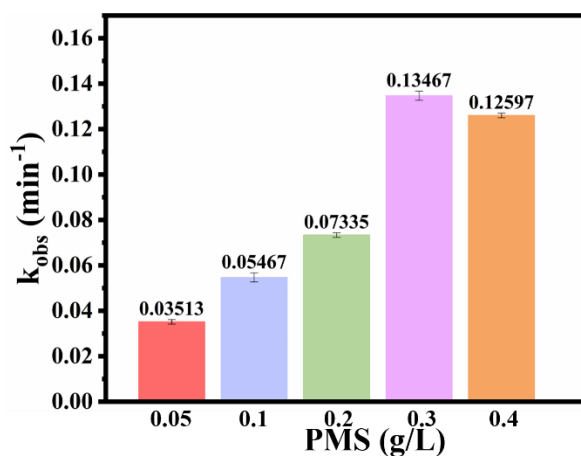
**Supplementary Figure 1.** Element mapping of Co/N@ZS-PDA.



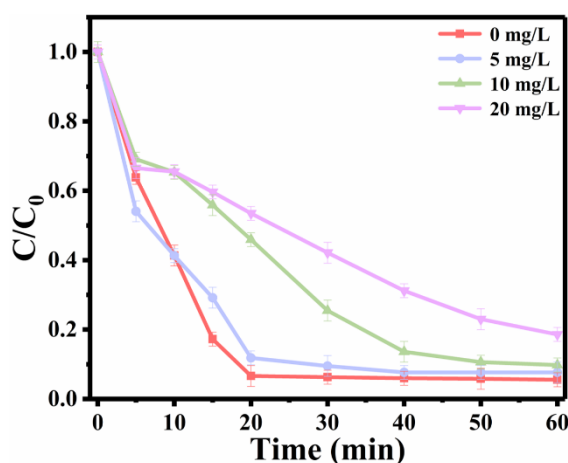
**Supplementary Figure 2.** Pseudo-first-order kinetic constant of different Catalysts. Each experiment was performed in triplicate, with error bars indicating the standard deviation of the results.



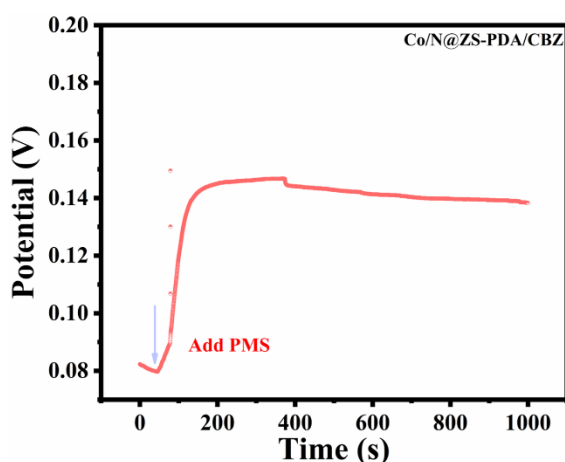
**Supplementary Figure 3.** Pseudo-first-order kinetic constant of different dosage of catalyst. Each experiment was performed in triplicate, with error bars indicating the standard deviation of the results.



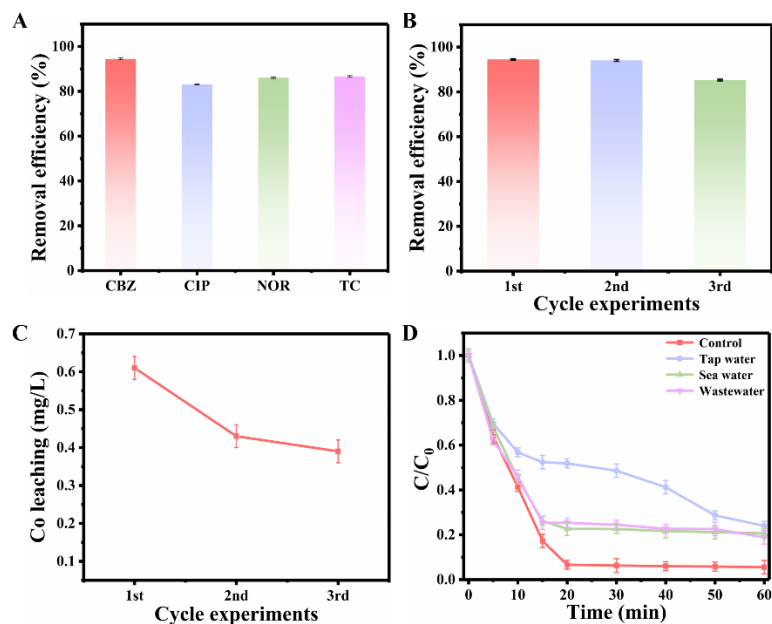
**Supplementary Figure 4.** Pseudo-first-order kinetic constant of different dosage of PMS. Each experiment was performed in triplicate, with error bars indicating the standard deviation of the results.



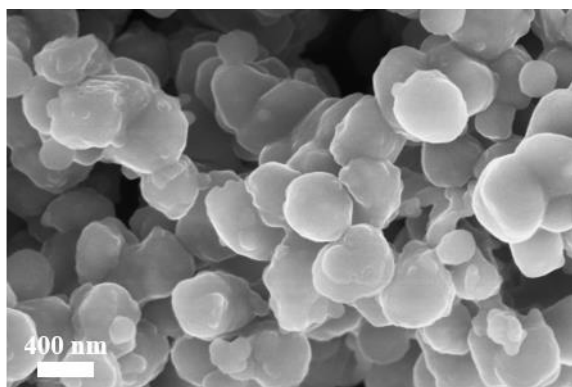
**Supplementary Figure 5.** Effect of HA on the CBZ degradation. Each experiment was performed in triplicate, with error bars indicating the standard deviation of the results.



**Supplementary Figure 6.** The open-circuit potential transients of Co/N@ZS-PDA



**Supplementary Figure 7.** (A) Degradation of different pollutants by Co/N@ZS-PDA; (B) the removal efficiency of CBZ in the cycle experiments; (C) ion leaching at different cycles; (D) effect of different water quality. Experimental conditions: [CBZ] = [CIP] = [NOR] = [TC] = 20 mg/L, [PMS] = 0.30 g/L, [Cat.] = 0.10 g/L. Each experiment was performed in triplicate, with error bars indicating the standard deviation of the results.



**Supplementary Figure 8.** The SEM images of the spent Co/N@ZS-PDA.



**Supplementary Figure 9.** Optical photographs of the practical device flow diagram in the dynamic degradation experiment.

## REFERENCES

1. Wu QY, Yang ZW, Wang ZW, Wang WL. Oxygen doping of cobalt-single-atom coordination enhances peroxymonosulfate activation and high-valent cobalt–oxo species formation. *Proc. Natl. Acad. Sci. U.S.A.* 2023, 120, 923120. DOI: 10.1073/pnas.2219923120.
2. Balta Z, Simsek EB. Discovering of the photocatalytic performance of BiFeO<sub>3</sub>/BNQDs immobilized polyester filters for efficient continuous-flow elimination of recalcitrant antibiotic via PMS activated process. *Opt. Mater.* 2022, 133, 113015. DOI: 10.1016/j.optmat.2022.113015.
3. Zhao X, An QD, Bo SF, et al. Highly Efficient Dynamic Degradation of Methylene Blue on Hierarchical Nitrogen/Cobalt-Co-Doped Carbonaceous Beads with Diffusion Promoting Nanostructures. *ChemNanoMat* 2019, 5, 802-813. DOI: 10.1002/cnma.201900145.
4. Bo S, Zhao X, An Q, Luo J, Xiao Z, Zhai S. Interior engineering of seaweed-derived N-doped versatile carbonaceous beads with Co<sub>x</sub>O<sub>y</sub> for universal organic pollutant degradation. *RSC Adv.* 2019, 9, 5009-5024. DOI: 10.1039/c9ra00357f.
5. Zhou M, Liu K, Peng Q, et al. Long-acting CoAl<sub>2</sub>O<sub>4</sub> spinel catalyst developed on activated alumina pellets by facile synthesis to activate peroxymonosulfate: Controllable cobalt leaching and environmental adaptability. *J. Environ. Manage.* 2022, 310, 114702. DOI: 10.1016/j.jenvman.2022.114702.